

The Yin-Yang dataset

L. Kriener¹, J. Göltz^{2,1}, M. A. Petrovici^{1,2}

¹Department of Physiology, University of Bern, 3012 Bern, Switzerland.

²Kirchhoff-Institute for Physics, Heidelberg University, 69120 Heidelberg, Germany.

Abstract

The Yin-Yang dataset was developed for research on biologically plausible error backpropagation and deep learning in spiking neural networks. It serves as an alternative to classic deep learning datasets, especially in algorithm- and model-prototyping scenarios, by providing several advantages. First, it is smaller and therefore faster to learn, thereby being better suited for the deployment on neuromorphic chips with limited network sizes. Second, it exhibits a very clear gap between the accuracies achievable using shallow as compared to deep neural networks.

1 Introduction

We introduce the Yin-Yang dataset for learning in hierarchical networks [1]. It is tailored to the requirements of research on biologically plausible error backpropagation algorithms, learning in spiking neural networks and deep networks on neuromorphic hardware. These fields typically require small but at the same time not trivially solvable datasets to prototype and test network architectures and learning algorithms. The datasets commonly used for this purpose are the MNIST and the fashion-MNIST datasets [2, 3]. However, these require comparatively large networks, considering the size of the visible layer alone. Despite this ostensible difficulty, they can nevertheless be classified with high accuracy even by shallow networks. This is problematic because training a deep network with an imperfect learning algorithm can result in performance undistinguishable from that of a shallow network. Conversely, a test on the MNIST dataset can fail to reveal the inability of the training algorithm to propagate error signals through the network, as the achieved high accuracies obscure the underlying problem.

The Yin-Yang dataset can provide an alternative for these testing and prototyping scenarios as it is solvable by smaller networks, contains fewer samples and most importantly exhibits a large gap between the accuracies reached by shallow and deep networks.

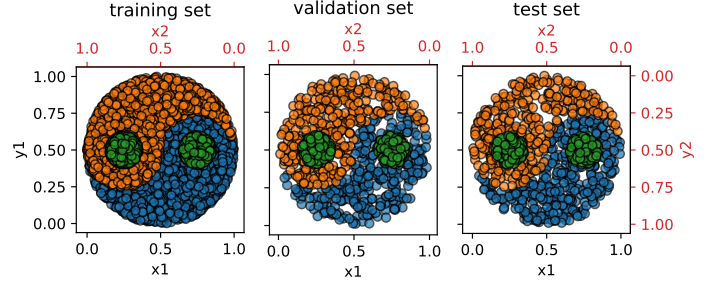


Figure 1: Training, validation and test dataset. Each dot in the yin-yang symbol represents one sample of the dataset. The color of the dot denotes its class (“Yin”, “Yang” or “Dot”). This figure was generated using the default settings for random seeds and dataset sizes (5000 samples for the training set and 1000 samples each for the validation and test set).

2 Dataset

Each sample in the dataset represents a point in a two dimensional representation of the yin-yang symbol. Depending on their location in the symbol the samples are classified into the “Yin”, “Yang” or “Dot” class (Fig. 1). Even though the areas in the yin-yang symbol covered by the different classes have different sizes, the dataset is designed to be balanced, which means that all classes are represented by approximately the same amount of samples. Note that therefore the density of samples is higher in the “Dot”-class regions, as the combined area of these regions is smaller than that of the others.

The samples are randomly generated using rejection sampling. The exact version of a generated set of samples is therefore determined by the random seed and dataset size. This makes it possible to produce multiple dataset versions by providing different random seeds and dataset sizes. In the default configuration the training set has 5000 samples while the validation and test sets have 1000 samples respectively, each generated with a different random seed.

As can be seen in Fig. 1, values of all samples in the dataset are strictly positive. This is the case to accommodate network models which require positive input values only (common in the field of biologically-plausible networks,

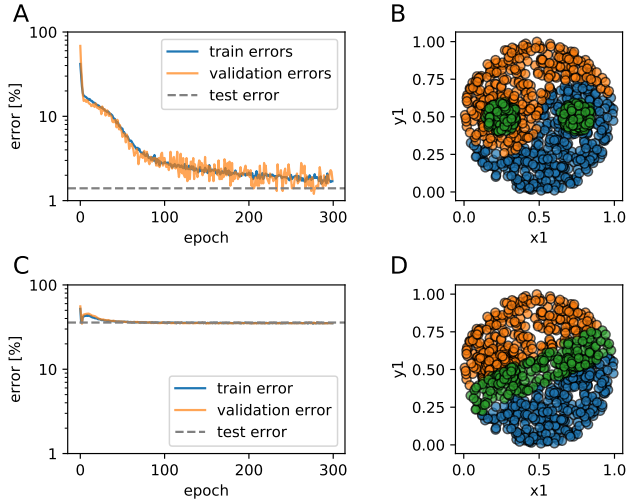


Figure 2: Comparison of training results for a deep versus a shallow network. Network parameters are given in Table 2. **A:** Evolution of the validation and training error during training of a deep neural network. The dashed line indicates the test error after 300 epochs of training. **B:** Training result of the deep network illustrated on the test set. Each sample is colored corresponding to the class determined by the trained network. **C:** Evolution of the validation and training error during training of a shallow neural network. **D:** Training result of the shallow network illustrated on the test set.

as firing rates as well as spike times are typically denoted by positive numbers). Because of that the yin-yang symbol is not centered around zero. This however complicates training in neuron models without intrinsic (learnable) bias. To facilitate training for these models, each sample in the dataset consists not only of the coordinates (x, y) determining the position in the yin-yang symbol but additionally also the values $(1 - x, 1 - y)$. This effectively symmetrizes the input and removes the need for a bias even though the yin-yang symbol is not centered around the origin of the coordinate system.

3 Training results

As a baseline for further applications of this dataset we also provide some training results achieved with classical artificial neural networks. The full set of training parameters can be found in Table 2. In particular, we compare the performances of a deep and a shallow network.

This comparison (Table 1 and Fig. 2) illustrates a manifest advantage of the Yin-Yang dataset compared to other commonly used datasets of comparable size: The shallow network is clearly unable to learn the required features to successfully classify the dataset, which leads to a gap of more than 30% between the accuracies achieved by a shallow and a deep network. This can be crucial in, for example, research on biologically plausible forms of error-

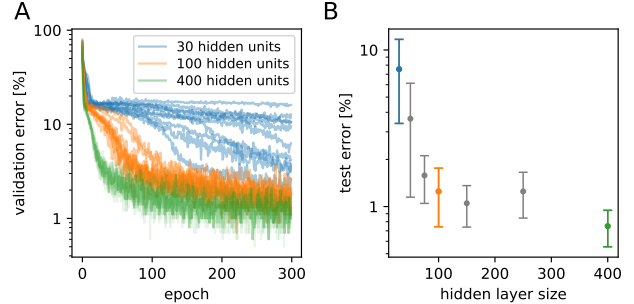


Figure 3: Impact of hidden layer size on network performance. **A:** Validation errors during training for three different network architectures with different hidden layer sizes. For each architecture, ten training runs with different random weight initialization are overlaid. **B:** Mean and standard deviation of the final test error depending on hidden layer size of the network. The colored data points correspond to the runs shown in A.

backpropagation, possibly even in spiking neural networks, as it requires the underlying learning algorithm to be able to harness the additional representational power of latent neuronal layers.

Another advantage of the Yin-Yang dataset over many other commonly used datasets is the dimensionality of its samples and the network sizes required to learn the task. Each sample consists of only four input values (compared to, e.g., the 784 input channels required by MNIST), which significantly reduces the required fan-in for hidden neurons. This can be especially beneficial on neuromorphic platforms, where the number of synaptic connections to a neuron is very often limited by the chip architecture. Also, this dataset can be learned with a single hidden layer of reasonably small size (Fig. 3). For consistently high final accuracies, a hidden layer of more than a hundred neurons is required, but for a small proof-of-concept demonstration of a learning algorithm or hardware prototype, even 30 hidden units are enough to achieve results that would be impossible with shallow networks, or with algorithms that cannot profit from a network’s representational hierarchy.

In addition to the results shown here, the dataset has already been used to showcase algorithms for error backpropagation in spiking neural networks in [4] and [5].

Table 1: Mean and standard deviation of training and test accuracy for 20 training runs with different random initializations. Training parameters can be found in Table 2.

network	test accuracy	training accuracy
deep network	$(98.7 \pm 0.3) \%$	$(98.5 \pm 0.3) \%$
shallow network	$(64.3 \pm 0.2) \%$	$(64.8 \pm 0.2) \%$

Table 2: Training parameters used to produce the results in Fig. 2. Fig. 3 uses the same parameters except for the size of the hidden layer.

parameter name	value
activation function	ReLU
size input	4
size hidden layer (for deep net)	120
size output layer	3
training epochs	300
batch size	20
optimizer	Adam, [6]
Adam parameter β	(0.9, 0.999)
Adam parameter ϵ	10^{-8}
learning rate	0.001

Code and data availability

Code for the Yin-Yang data set is available at https://github.com/lkriener/yin_yang_data_set. The example notebook in the repository includes the plotting of the data samples (Fig. 1) and the training of deep and shallow networks (Fig. 2). Additional data available on request from the authors.

References

1. *Yin-Yang dataset repository* https://github.com/lkriener/yin_yang_data_set. Accessed: 2021-01-20.
2. LeCun, Y., Bottou, L., Bengio, Y. & Haffner, P. Gradient-based learning applied to document recognition. *Proceedings of the IEEE* **86**, 2278–2324 (1998).
3. Xiao, H., Rasul, K. & Vollgraf, R. Fashion-mnist: a novel image dataset for benchmarking machine learning algorithms. *arXiv:1708.07747* (2017).
4. Göltz, J. et al. Fast and deep: energy-efficient neuromorphic learning with first-spike times. *arXiv:1912.11443* (2019).
5. Wunderlich, T. C. & Pehle, C. EventProp: Back-propagation for Exact Gradients in Spiking Neural Networks. *arXiv:2009.08378* (2020).
6. Kingma, D. P. & Ba, J. Adam: A Method for Stochastic Optimization. *arXiv:1412.6980* (2014).

Acknowledgment

We wish to thank Sebastian Billaudelle and Benjamin Cramer for valuable discussions, as well as Mike Davies and Intel for their ongoing support. We gratefully acknowledge funding from the European Union under grant agreements

604102, 720270, 785907, 945539 (HBP) and the Manfred Stärk Foundation.

During the development of the dataset some calculations were performed on UBELIX, the HPC cluster at the University of Bern, others were performed on the bwForCluster NEMO, supported by the state of Baden-Württemberg through bwHPC and the German Research Foundation (DFG) through grant no INST 39/963-1 FUGG. Additionally, our work has greatly benefitted from access to the Fenix Infrastructure resources, which are partially funded from the European Union’s Horizon 2020 research and innovation programme through the ICEI project under the grant agreement No. 800858.